crystals

MDPI

Article

Technology and Dielectric Properties of BLT4 Ceramics Modified with Special Glass

Beata Wodecka-Dus [1], Jolanta Makowska [1,*], Tomasz Pikula [2], Rafał Panek [3], Małgorzata Adamczyk-Habrajska [1] and Katarzyna Osińska [1]

[1] Faculty of Science and Technology, Institute of Materials Engineering, University of Silesia, 75 Pułku Piechoty 1A, 41-500 Chorzow, Poland; beata.wodecka-dus@us.edu.pl (B.W.-D.); malgorzata.adamczyk-habrajska@us.edu.pl (M.A.-H.); katarzyna.osinska@us.edu.pl (K.O.)
[2] Institute of Electronics and Information Technology, University of Technology, 38A Nadbystrzycka Street, 20-618 Lublin, Poland; t.pikula@pollub.pl
[3] Department of Construction Materials Engineering and Geoengineering, Lublin University of Technology, 40 Nadbystrzycka Street, 20-618 Lublin, Poland; r.panek@pollub.pl
* Correspondence: jolanta.makowska@us.edu.pl; Tel.: +48-32-2691841

Abstract: Lead-boron special glass was doped into $Ba_{0.996}La_{0.004}Ti_{0.999}O_3$ (BLT4) ceramics in order to control the sintering process and grain growth, consequently obtaining materials with a well-developed microstructure. Changes in the microstructure resulted in a significant decrease in electrical permittivity along with a substantial increase in its frequency dispersion. Glass-doped ceramics, similar to pure BLT4, are characterized by a first-order phase transition from the ferroelectric phase to the paraelectric phase. The temperature of this transition shifts slightly towards higher values with the increase in glass dopant concentration.

Keywords: $Ba_{1-x}La_xTi_{1-x/4}O_3$ ceramics; special glass; dielectric properties

Citation: Wodecka-Dus, B.; Makowska, J.; Pikula, T.; Panek, R.; Adamczyk-Habrajska, M.; Osińska, K. Technology and Dielectric Properties of BLT4 Ceramics Modified with Special Glass. *Crystals* **2024**, *14*, 739. https://doi.org/10.3390/cryst14080739

Academic Editor: Zhonghua Yao

Received: 2 August 2024
Revised: 16 August 2024
Accepted: 19 August 2024
Published: 20 August 2024

1. Introduction

Barium lanthanum titanate $Ba_{1-x}La_xTi_{1-x/4}O_3$ is an advanced ceramic material that is widely used due to its unique dielectric and ferroelectric properties [1–4]. Particularly noteworthy are ceramics containing 0.4 mol.% lanthanum $Ba_{0.996}La_{0.004}Ti_{0.999}O_3$ (BLT4), which shows a huge value of electrical permittivity, with a relatively low level of dielectric losses, piezoresistive and semiconductor properties at room temperature, and, above the Curie temperature, posistor properties and piezoelectric properties [5–7]. This allows us to assume that BLT4 ceramics can be used as an alternative filling in ultracapacitors and could constitute a base material for potential applications in piezoresistive pressure sensors, PTCR thermistors, and piezoelectric sensors [8–10]. Currently, there is a significant need and strong demand for new generation electrical energy storage devices, in which high dielectric constant and low dielectric losses and high dielectric breakdown strength of materials play a key role [11–13].

Unfortunately, ferroelectric ceramic materials exhibiting high dielectric permittivity and relatively low dielectric losses are also characterized by low dielectric breakdown strength. Several external factors contribute to this phenomenon, such as pores, grain boundaries, and anisotropic permittivity in randomly oriented crystals [14,15]. A promising material to eliminate the above defect may be special glass, which has high thermal stability and high dielectric breakdown strength, which makes it a candidate for use in high-temperature energy storage capacitors [16–18]. Glass-forming components as sintering additives create an irregular liquid phase during sintering, which causes good wettability at the grain boundary [19–21]. By acting as a sintering activator, they contribute to improving technological conditions and, above all, to lowering the optimal sintering temperature [22], which leads to energy savings and lowers the costs of the production process. By reducing

the porosity of the ceramics, the addition of glass increases its density and also increases its mechanical strength by reducing internal mechanical stresses. The admixture of special glass also affects the purification of crystallites by the diffusion of "foreign" atoms into the glassy phase and reduces the effects of evaporation of volatile components, while the crystal grains increase the degree of angularity [23].

In this work, a lead-boron special glass from the PbO-B_2O_3-Al_2O_3-WO_3 system was selected as the sintering activator. The composition of the glass-forming agent was dictated by many important considerations. Glassy materials, which consist of the heaviest metal oxides, such as lead, are more promising for photonics and optoelectronics. Depending on the type of bond, ionic or covalent between lead and oxide, respectively, PbO plays the role of a modifier or glassy agent [24]. Lead oxide significantly reduces viscosity, especially at high temperature, and reduces surface tension, thereby improving electrical properties of glasses. In addition, PbO is a binder, preventing lead evaporation, melts at T = 1161 K, and is not classified as a glass-forming agent, but easily forms glass with B_2O_3 [25]. Boron trioxide B_2O_3 is one of the most important components of glasses. It has strong glass-forming properties and easily forms glasses with many oxides. B_2O_3 improves the electrical insulating properties of glasses (high resistance, low dielectric losses) and significantly increases hardness but reduces the density of glass. It is a relatively volatile component and melts at T = 1073 K [26,27]. Boron glasses are among the most well-known and unique glass systems. They have useful optical, thermal, and electrical applications, and have recently been used as potential bioactive candidates [28]. One of the most important components of glasses, giving them several advantageous properties, is undoubtedly Al_2O_3. It increases the mechanical strength, hardness, surface tension, and electrical conductivity of glass. It forms a liquid phase during sintering, lowers the temperature of eutectic formation with $BaTiO_3$, and increases the grain size (from 2 to 8 μm) [29]. WO_3-based glasses, which exhibit significant nonlinearity and electrical characteristics, have become increasingly important technologically over the years, despite the occurrence of electro- and photochromic phenomena [30–32]. Tungsten trioxide is classified as an oxide catalyst for crystallization (devitrification), increases the density of glass, and is a surface-active component—it has a significant effect on surface tension. The special features of tungsten trioxide, such as the field intensity and high valence of tungsten (VI), promote network formation and improve mechanical properties [33]. Tungsten oxide has many innovative applications, including the production of "smart windows", anti-reflective rear-view mirrors for cars, zero-emission displays, optical recording systems, and can act as a gas, humidity and temperature sensor in the solid state [34]. Due to the ability to create large areas of glass and change its oxidation from three to four, B_2O_3 is a very suitable host for the introduction of metal ions. In addition, the size of ions in the glass network, the movement of the modifier cation, and other factors have a significant effect on the degree and ability to include WO_3 in glasses [35]. By creating new strong bonds with tungsten, lead-boron special glasses containing an appropriate concentration of WO_3 cause an increase in the dielectric constant and conductivity with increasing temperature, revealing the semiconducting behavior of the samples [36]. This predisposes them for applications in a broadly understood group of electronic devices.

The use of lead-boron special glass, whose properties have been widely studied and described by the authors [24,37], as a modifier of ferroelectric ceramics contributes to lowering the sintering temperature, thereby improving the material consolidation process. Thanks to the glassy phase, ceramics with well-developed intergranular boundaries and large angular grains, the best stoichiometry and a high degree of perfection of the crystal structure were obtained. It also allowed the dielectric to transition into the semiconductor state and then into the posistor state and obtain the PTCR effect above the Curie temperature. In the context of dielectric properties, the admixture of lead-boron glass can lead to a reduction in dielectric losses and an improvement in the temperature stability of ceramics [38,39]. To sum up, an admixture of special glass introduced into ferroelectric ceramics can have a multi-faceted impact on its properties. Optimizing these properties requires precise

selection of the type and quantity of glass, as well as control of the production process to obtain the desired results in the context of a specific application.

Research on the influence of the admixture of lead-boron glass on the properties of $Ba_{0.996}La_{0.004}Ti_{0.999}O_3$ ceramics, which is an advanced electroceramic material with unique dielectric and ferroelectric properties, is crucial for a better understanding of the interactions between the glassy and ceramic phases and for the development of new materials with improved parameters [36,40–42]. This approach may contribute to the development of advanced technologies, including modern electronic devices such as electromagnetic wave absorbers. These devices play an important role in today's world, which is filled with electromagnetic noise. Particularly valued are absorbers made from ceramic materials due to their resistance to weather conditions and, consequently, their ability to operate outdoors. So far, ceramic absorbers based on titanite, which has a very low dielectric permittivity, have been developed. They are used in the millimeter-wave frequency range. Ferroelectric ceramics, whose permittivity is at least 100 times greater, have significant application potential in this regard [43,44]. With suitably controlled dielectric dispersion, it is possible to create electromagnetic wave absorbers that operate in any frequency band. One of the ceramic materials considered is barium titanate [45,46]. Attempts have been made to change the frequency dispersion range of the electric permittivity by doping it with strontium or calcium [47,48]. However, the range of changes was small. Similar effects were achieved with dopants such as B, Li, and Na [45]. In this paper, we report, among other things, the effect of adding special glass dopants on the frequency dispersion of electric permittivity, as well as its impact on the microstructure, crystalline structure, and dielectric properties.

2. Materials and Methods

The technological process of obtaining barium lanthanum titanate (BLT4) ceramics modified with special glass consisted of three basic stages. The first stage involved obtaining lead-boron glass containing W^{6+} cations. The preparation of special glass as a modifying admixture was made by melting a mixture of simple oxides of high purity (99.99%, Sigma-Aldrich, USA, St. Louis MO) in the following amounts by weight: PbO (73.4 wt%), B_2O_3 (18.4 wt%), Al_2O_3 (5.2 wt%), and WO_3 (3.0 wt%). These substrates were mixed together in a planetary ball mill for t = 24 h and then melted in a corundum crucible at T = 900 °C for t = 1 h. The alloy was poured onto a steel plate for rapid cooling and devitrification. The obtained glass was crushed and ground into powder in a mortar for approximately t = 1 h and in this form it was added to BLT4 ceramics as a modifying admixture. The second stage of the technology was related to the synthesis of BLT4 ceramics by donor doping of pure barium titanate (BT) with lanthanum La^{3+} ions in an amount of 0.4 mol.%. The starting materials for obtaining BLT4 ceramics using the conventional method were analytically pure compounds: barium carbonate, lanthanum oxide, and titanium (IV) oxide (99.99%, Sigma-Aldrich, St. Louis, MO, USA). The substrates were weighed in a stoichiometric ratio, taking into account the expected chemical reaction (1):

$$(1 - x)BaCO_3 + (1/2x)La_2O_3 + (1 - x/4)TiO_2 \rightarrow Ba_{1-x}La_xTi_{1-x}/4O_3 + (1 - x)CO_2\uparrow \quad (1)$$

In this way, powders with the desired composition were obtained, which can be represented by a schematic reaction Equation (2):

$$0.996BaCO_3 + 0.002La_2O_3 + 0.999TiO_2 \rightarrow Ba_{0.996}La_{0.004}Ti_{0.999}O_3 + 0.996CO_2\uparrow \quad (2)$$

The prepared powders were dry mixed in a porcelain mortar for t = 1 h and then prepared for wet grinding with the addition of ethyl alcohol C_2H_5OH (99.99%, POCH, Poland, Gliwice) in a planetary ball mill, using zirconium-yttrium balls as grinding media. Based on thermal analyses [5], the synthesis was carried out at a temperature of T_S = 950 °C for t = 2 h. After heat treatment, the moldings were crushed and ground. The third stage concerned the introduction of an admixture of special glass from the PbO-B_2O_3-Al_2O_3-WO_3

system in amounts of 2, 4, 6, and 8 by weight % to the basic composition of BLT4 ceramics. The modified compositions were pre-ground in porcelain mortars for t = 1 h and then subjected to wet mechanical mixing using a suspension with the addition of ethyl alcohol and ceramic grinders with a diameter of d = 10 mm made of zirconium oxide stabilized with yttrium oxide, the number of which was selected in proportion to the mass of the ground powder. The mixing process was carried out in a planetary ball mill for t = 24 h at 250 rpm. Powders of oxide mixtures homogenized in this way were dried in air until the alcohol completely evaporated.

In order to select appropriate technological conditions for the modified powders, thermal analysis was carried out using the thermogravimetric method (TG) and differential thermal analysis (DTA), and in parallel, differential thermogravimetric analysis (DTG) was also performed. Measurements were performed for all compositions using a MOM Q-1500D derivatograph (Paulik-Paulik-Erdey System, Budapest, Hungary). Based on detailed thermal analysis tests, optimal technological conditions were adopted for BLT ceramics modified with special glass.

Before the sintering process, the obtained powders were pressed by unilateral, uniaxial cold pressing on a hydraulic press at a pressure of p = 300 MPa in a steel die with a diameter of d = 10 mm. The finished ceramic moldings were placed in corundum crucibles with Al_2O_3 (99.99%, Sigma-Aldrich, St. Louis, MO, USA) bedding and the first sintering was carried out in an electric resistance furnace—HTC 1500 at T_1 = 1250 °C for t = 2 h. The crushing, grinding, and pressing procedure was then repeated. Final sintering was carried out at T_2 = 1300 °C for t = 2 h. During sintering, the controller recorded the temperature and operating time of the furnace. The temperature rise rate in the furnace was t = 5 °C/min. The ceramic samples obtained as a result of the technological process were mechanically processed, consisting of grinding and polishing to a thickness of approximately 1 mm. Then, the samples were dried at T = 373 K for t = 1 h and annealed by quick heating to T = 873 K and slow cooling to remove internal stresses.

The structure of the prepared samples (phase composition) was investigated using the X-ray diffraction (XRD) method with a Panalytical X'pert PRO MPD diffractometer (Eindhoven, The Netherlands) operating in the standard Θ–2Θ mode. The diffractometer was equipped with a PW 3050 goniometer, PIXcel 1D raster detector, and a copper (Cu) lamp (CuKα = 1.54178 Å). The HighScore Plus program with a PDF-2 DL database (2022 edition) formalized by JCPDS-ICDD was used for the phase and structural analyses.

The manufactured ceramic materials were also subjected to microstructural analysis performed using a SEM JEOL JSM-7100F TTL LV (Akishima, Japan) scanning electron microscope.

Measurements of dielectric properties were carried out on specially prepared samples, using a computerized measurement system, an integral part of which was the Agilent E4980A LCR meter (Santa Clara, CA, USA). The samples used for dielectric measurements were disc-shaped with a thickness of 0.6 mm and a surface area of 1 cm^2. Conductive silver paste (P-120, supplier: Polish State Mint, Warsaw, Poland) was applied to the parallel surfaces using the burning method. Before the actual measurements, the samples were heated at T = 400 °C for t = 30 min to reduce the stresses caused by previous mechanical processing. This process also resulted in the relaxation of initially immobile defects formed during the sintering process.

3. Results

3.1. Thermal Analysis

All powders, in the form of 50 mg weighed, were subjected to thermal analysis before undergoing the synthesis process using the following methods: thermogravimetric (TG) and differential thermal analysis (DTA). As is known, the quantity measured in the thermogravimetric method is the change in mass, while differential analysis determines the temperature difference between the sample and the standard, most often in the form of pure Al_2O_3. Since the reference substance, which is aluminum oxide, is not subject to transformations accompanied by thermal effects, the measured difference ΔT depends on

the rate of heat absorption or release by the samples. In order to improve the readability of the TG curve, differential thermogravimetric (DTG) analysis was performed in parallel. As a result, next to the TG curve, its first derivative with respect to temperature (T) was obtained. The recorded total weight loss of the sample was equal to the area of the TG peak on this curve. Thermal analysis of the tested compositions was carried out in the temperature range T = (20 ÷ 1000) °C in an air atmosphere. The temperature increase rate was v = 10 deg/min. Figure 1 shows the TG, DTG, and DTA thermal curves for the as-synthesized BLT4 ceramic powder, glass powder, and glass-doped BLT4 ceramic powder.

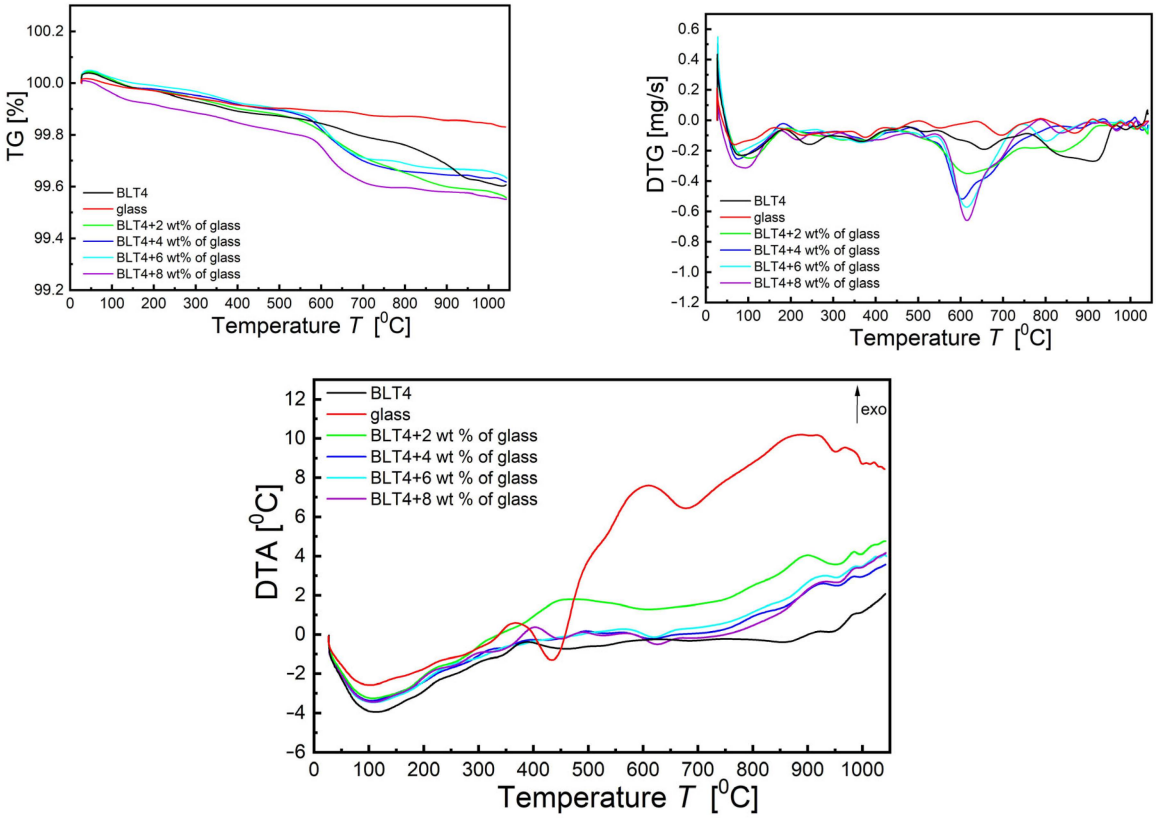

Figure 1. Thermal behavior of the substrate mixture of pure BLT4 ceramics, special glass, and BLT4 ceramics doped with special glass after synthesis.

In the TG curves for all compositions, it is observed that the total mass loss is Δm = 0.4%. As the glass content in the tested material increases, the mass loss increases. Two temperature ranges corresponding to mass losses can be observed on the TG thermal curves. The first mass loss at ΔT_1 = (20–150) °C is accompanied by a minimum in the DTG curves at a temperature of approximately T = 80 °C and an endothermic maximum (minimum in the curves) in the DTA curves at a temperature of approximately T = 100 °C. The first observed weight loss is related to the evaporation of moisture from the powders. The second mass loss, for pure and glass-doped BLT4 ceramic powders, occurring in the temperature range ΔT_2 = (550–750) °C, is accompanied by a minimum on the DTG curves at a temperature of approximately T = 600 °C for doped compositions and at a temperature of approximately T = 650 °C for pure BLT4 and a small endothermic maximum in the DTA curves around the temperature T = 650 °C appearing for doped compositions. As the glass content in the tested material increases, this maximum becomes more and more visible. This maximum is responsible for the formation of intermediate phases during the transformation of perovskite. In the case of TG and DTG thermal curves, their courses for glass and BLT material doped with glass are similar. However, DTA curves have a completely different course for pure glass. The DTA curve shows typical transformations occurring in glassy materials. The endothermic maximum (minimum on the curve) occurring on the

DTA curve at T = 100 °C is related to the evaporation of moisture from the powdered glass. As the temperature increases, an inflection point is observed around T_g = 370 °C, associated with the beginning of the glass softening process. However, the endothermic maximum at T_d = 430 °C is the glass softening temperature. The large exothermic maximum on the DTA curve, observed at T_c = 610 °C, is responsible for the crystallization of the glass. During further heating of the glass, the crystallized phase melts, observed on the DTA curve in the form of an endothermic maximum at T_m = 680 °C.

3.2. X-ray Analysis

Figure 2 shows the XRD patterns recorded for all the investigated BLT4 samples. The top panel of Figure 2 depicts the diffractogram taken for the glass powder used in the synthesis process. One can note two broad peaks characteristic of amorphous materials in the case of the glass sample. No crystalline phases were detected.

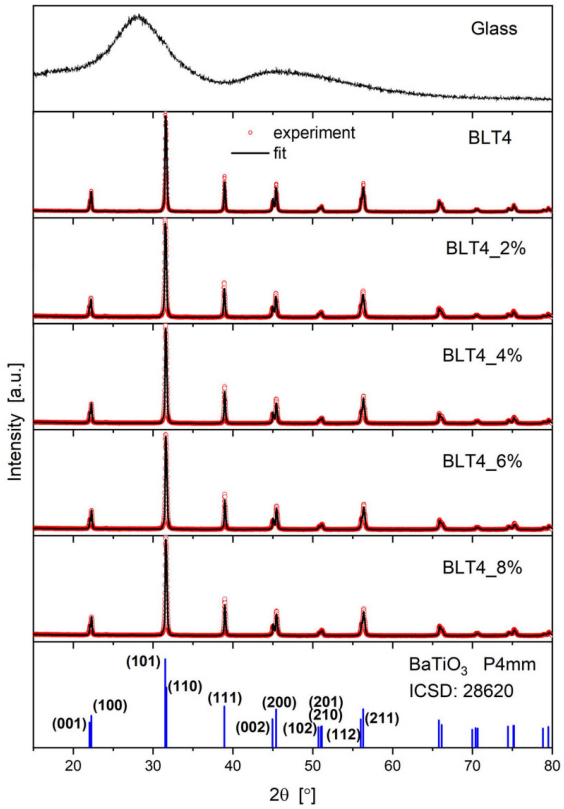

Figure 2. The results of XRD analyses for BLT4 ceramics modified with special glass. The top panel shows the diffractogram registered for the special glass used in the synthesis procedure. The bottom panel shows the standard room temperature XRD pattern for tetragonal $BaTiO_3$ (ICSD code 28620) as a reference.

In the case of the investigated composites, pure BLT4 phases were obtained without any secondary phase. Interestingly, it can be noted that the background is flat and there is no trace of an amorphic glass-like phase. Thus, it can be stated that the glass elements were incorporated into the perovskite lattice of BLT4. This finding is confirmed by the DTA results, which show no features typical for glass in the case of all glass-doped BLT4 samples, and DTG data showing a growth of the height of the exothermic minimum at T = 600 °C with increasing concentration of glass. The structure of all the samples was found to be tetragonal (P4mm space group), characteristic of the pure $BaTiO_3$ compound at room temperature. The bottom panel of Figure 2 shows the positions and intensities of diffraction peaks reported for the $BaTiO_3$ compound (ICSD No.: 28620) as a reference. The

Rietveld method was used for refinement of the unit cell of the obtained BLT4 samples. Structural parameters were derived and summarized in Figure 3.

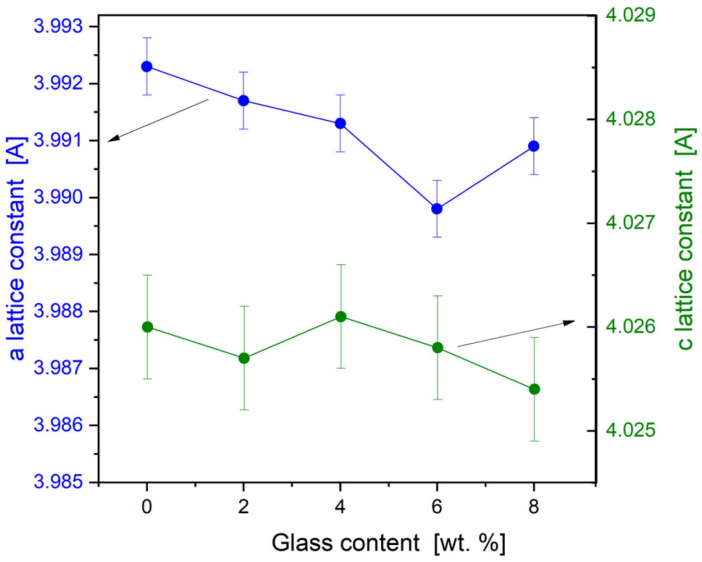

Figure 3. Lattice parameters of BLT4 ceramics modified with special glass derived from Rietveld refinement of tetragonal P4mm unit cell as a function of special glass content.

It can be noted that the *c* lattice constant was weakly sensitive to the contribution of glass in the composite and it is close to 4.026 Å. On the other hand, the parameter *a* slowly decreases, reaching a minimum of around 3.990 Å for sample BLT4_6%, and then increases to 3.9909 Å for BLT4_8%. This proves that the glass elements were incorporated into the BLT lattice, thereby slightly modifying the unit cell parameters. The decrease of *a* lattice constant and a drop of a unit cell volume can be attributed to the partial substitution of titanium by tungsten, as was reported earlier in [38].

3.3. Scanning Electron Microscopy

Fractured samples were used for microstructural tests of the surface of the manufactured ceramics. Samples for analysis were initially cleaned of micropollutants with acetone (p.a.) using an ultrasonic scrubber. Then, using a carbon sputter (turbomolecular), they were covered with a thin layer of gold to facilitate the removal of electrons from the tested surface. Samples prepared in this way were placed on the stage of a scanning electron microscope. Figure 4 shows SEM images of the fracture surfaces of pure BLT4 ceramics and for various concentrations of the special glass admixture introduced at a magnification of 10,000×.

Literature data indicate that the ideal microstructure of doped $BaTiO_3$ ceramics should be characterized by well-formed, homogeneous grains of barium titanate containing dissolved donor dopants [49]. For BLT4 0% ceramics, the appearance of the microstructure indicates that fractures occurred through the grains (transgranular fractures) during the breaking process. The obtained ceramics are characterized by well-formed large prismatic grains, with a tendency for spiral hexagonal growth. This two-dimensional grain growth mechanism significantly increases the size of individual grains, consequently enhancing the strength of the obtained ceramics [49]. With the increase in the content of the special glass additive, a decrease in grain size is observed. Additionally, it can be noted that the grains are prismatic and more densely packed. The surface microstructure is not homogeneous; it features areas of both coarse and fine grains. The presented images of the fracture microstructure clearly indicate that the fractures characteristic of the studied materials are intergranular fractures. This suggests a positive impact of the special glass additive on grain quality.

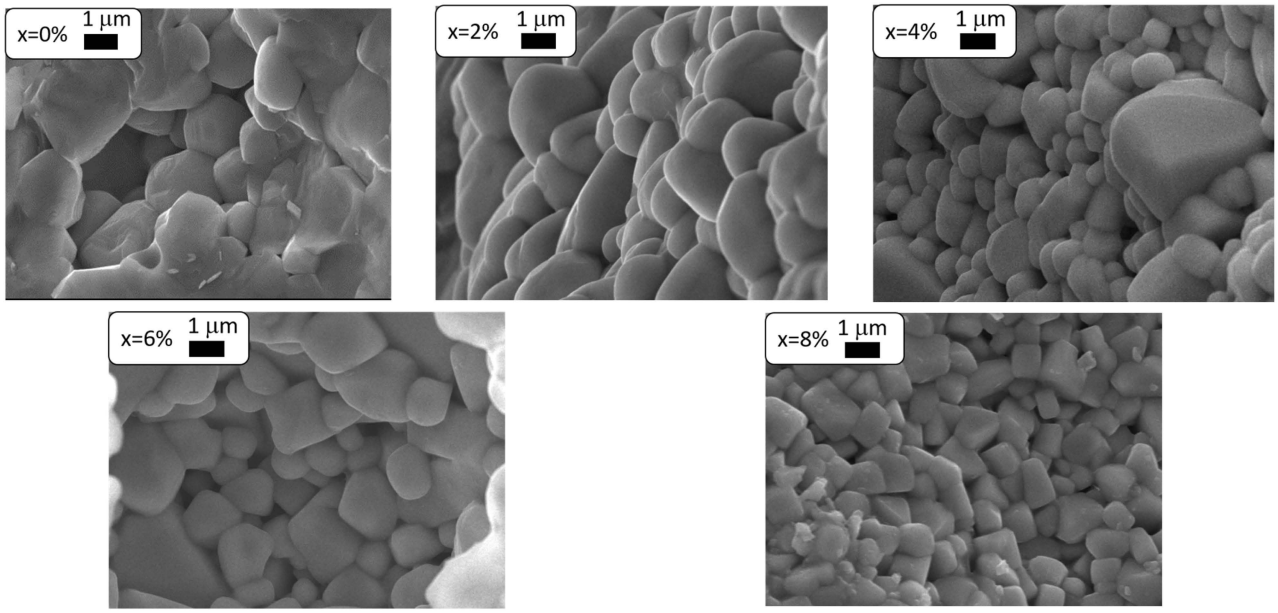

Figure 4. SEM photos of ceramic fractures.

3.4. Dielectric Properties

In the first step of analyzing the influence of special glass additives on the properties of BLT4 ceramics, the temperature dependencies of the dielectric constant and the tangent of the loss angle were measured in a measurement field with an amplitude of 1 V and a frequency of 1 kHz. The obtained characteristics are presented in Figure 5.

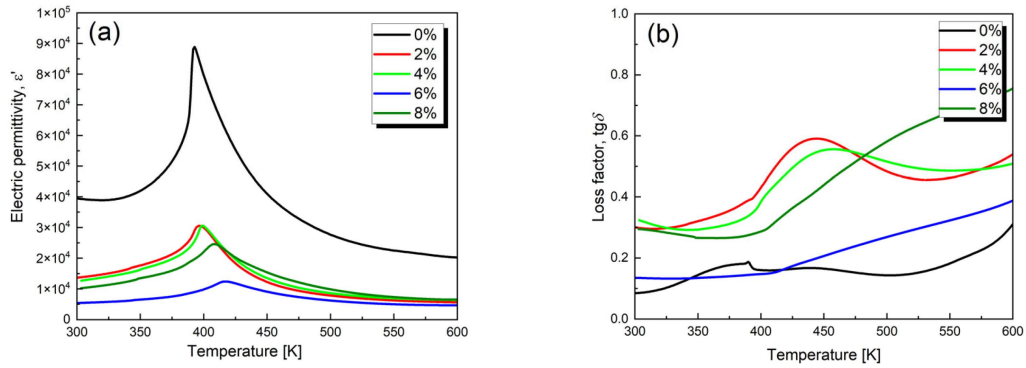

Figure 5. Dielectric permittivity (**a**) and dielectric loss tangent (**b**) as a function of temperature, measured at frequency 1 kHz on heating processes for pure BLT4 ceramics and those modified with special glass.

The modifying additive in the form of lead-boron special glass introduced into lanthanum barium titanate ceramics significantly reduced the maximum value of the dielectric constant, from ε_{max} = 99,140 for pure BLT4 ceramics to ε_{max} = 12,407 for BLT4 + 6% glass. Further increasing the concentration of the modifier (up to 8% glass) causes a subsequent twofold increase in the dielectric constant, both at room temperature and at the Curie temperature (Table 1). However, it should be emphasized that all the discussed ceramic materials are characterized by high dielectric constant values (both at room temperature and at the phase transition temperature) while maintaining low values of the dielectric loss tangent, which is extremely important from an application perspective (Table 1). According to the authors of the study [37], such low tan delta values may be due to the decreasing pore content. In the paraelectric phase region, a slight increase in tgδ is observed, which is related to the increase in electrical conductivity caused by the rise in temperature.

Table 1. The influence of the amount of special glass on the dielectric parameters of BLT4 ceramics determined at a measurement field frequency of f = 1 kHz.

Special Glass Content	T_C [K]	ε_{RT}	ε_{max}	tgδ_{RT}	tgδ_{TC}	T_0 [K]	C [K]
0%	393	39,497	99,140	0.08	0.20	348	4.20×10^5
2%	397	13,391	30,530	0.31	0.41	369	9.97×10^5
4%	399	12,670	30,578	0.32	0.38	365	1.16×10^6
6%	417	5363	12,407	0.13	0.16	342	9.80×10^5
8%	408	10,222	24,593	0.29	0.31	356	1.42×10^6

With the increase in the amount of glass in the studied materials, a gradual shift towards higher Curie temperature values is observed, from T_C = 393 K for BLT4 ceramics to T_C = 417 K for BLT4 + 6% glass, followed by a decrease in T_C for a glass concentration of 8%. According to the authors of the paper [13], the reason for this behavior can be attributed to the compositional variation in the ferroelectric phase caused by the incorporation of elements between the ceramic and glass phases.

The shape of the reciprocal of electric permittivity in the function of temperature for all discussed ceramics shown in Figure 6 points to the sharp transition between the ferro- and paraelectric phase occurring at T_C. Moreover, the discussed dependencies follow the Curie–Weiss law at temperatures above temperature T_C. According to the mentioned relationship, the Curie–Weiss temperature (T_0) and constants were obtained from linear extrapolation of $1/\varepsilon$ (T) characteristics in the high-temperature region (Table 1).

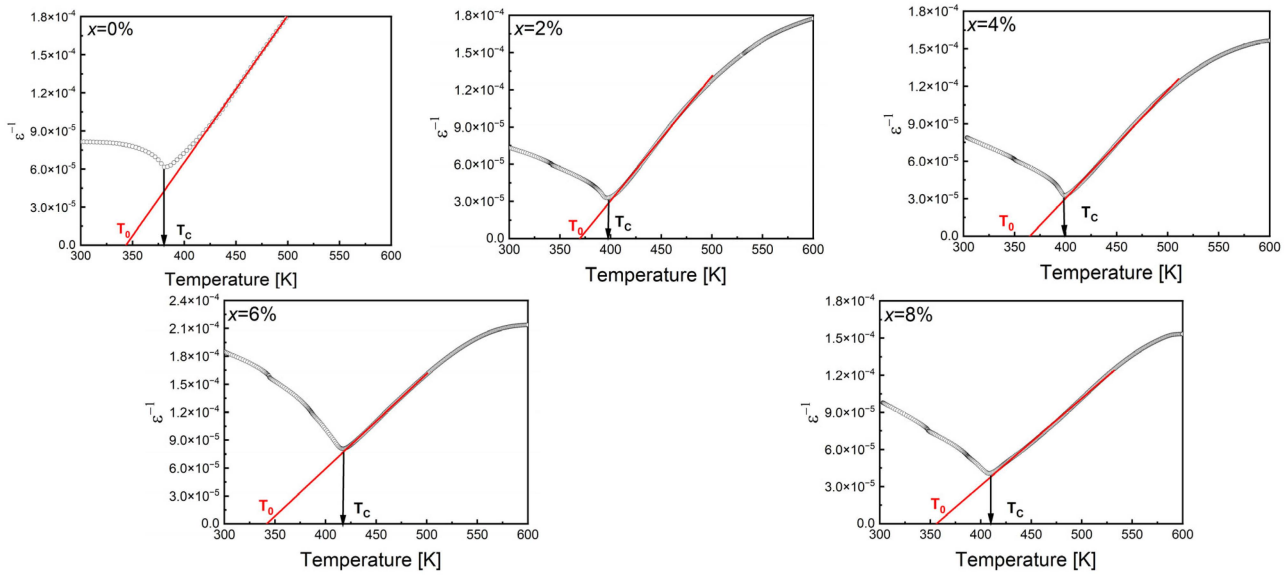

Figure 6. The reciprocal permittivity ($1/\varepsilon$) at 1 kHz as a function of temperature for pure BLT4 and BLT4 ceramics modified with special glass.

The obtained Curie–Weiss temperatures are lower than T_C, and the difference between temperature T_C and T_0 is significant (about 28–75 K). From the above results, it is clear that first-order phase transitions occur in pure BLT4 ceramics as well as in the modified ones.

Considering the potential application of glass-modified ceramic materials BLT4 in electromagnetic wave absorbers, the temperature dependencies of electrical permittivity were measured at several selected field measurement frequencies ranging from 100 Hz to 1 MHz. The obtained curves clearly indicate the presence of significant frequency dispersion of electrical permittivity noticeable across the entire range of investigated temperatures for all discussed materials. To quantitatively define the influence of special glass on the mentioned

dispersion, its measure was determined as the difference between the maximum values of electrical permittivity measured for the two extreme field measurement frequencies, denoted as $\Delta\varepsilon_{max}$. In the case of pure barium lanthanum titanate ceramics, this difference is the smallest and amounts to $\Delta\varepsilon_{max}$ = 22,239, which constitutes 25% of the maximum value of electrical permittivity measured in a field of frequency f = 100 Hz.

With an increase in the concentration of lead-borate special glass in BLT4 ceramics, there is a distinct increase in frequency dispersion, and for ceramics with the highest amount of glass additive, it reaches $\Delta\varepsilon_{max}$ = 30,015, which constitutes as much as 87% of ε_{max} at frequency 100 Hz. Similar results were obtained for values of frequency dispersion at room temperature (see Table 2).

Table 2. Quantitative description of the frequency dispersion observed in pure BLT4 ceramics as well as in ceramics modified with special glass at room temperature ($\Delta\varepsilon_{RT}$) and at the Curie temperature ($\Delta\varepsilon_{max}$).

Special Glass Content	$\Delta\varepsilon_{RT}$	$\Delta\varepsilon_{max}$
0%	4387 (10%)	22,239 (25%)
2%	16,331 (85%)	41,512 (83%)
4%	14,971 (86%)	38,510 (84%)
6%	4727 (75%)	11,395 (74%)
8%	12,514 (88%)	30,015 (87%)

The sources of frequency dispersion should be sought in the increasing contribution of space charge within the sample volume and its polarization. It is also worth noting that the Curie temperature T_C remains unchanged, which clearly excludes the presence of properties typical for ferroelectric relaxers [50]. Strong frequency dispersion of electrical permittivity is accompanied by dispersion of the dielectric loss tangent, which is also observed across the entire considered temperature range. However, the value of tanδ remains very low (see Figure 7).

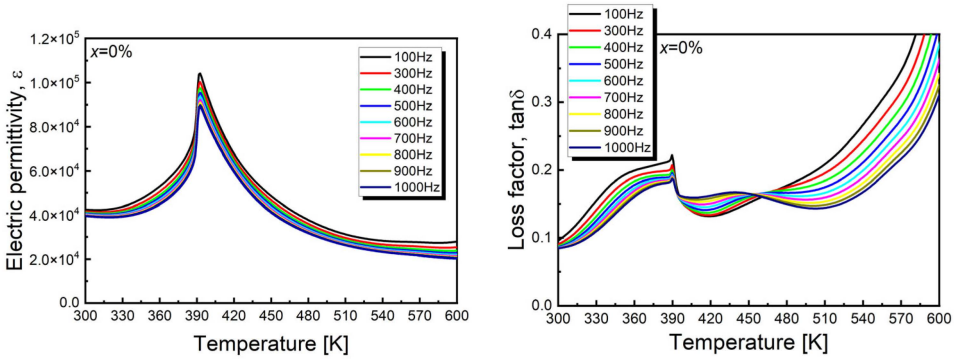

Figure 7. *Cont.*

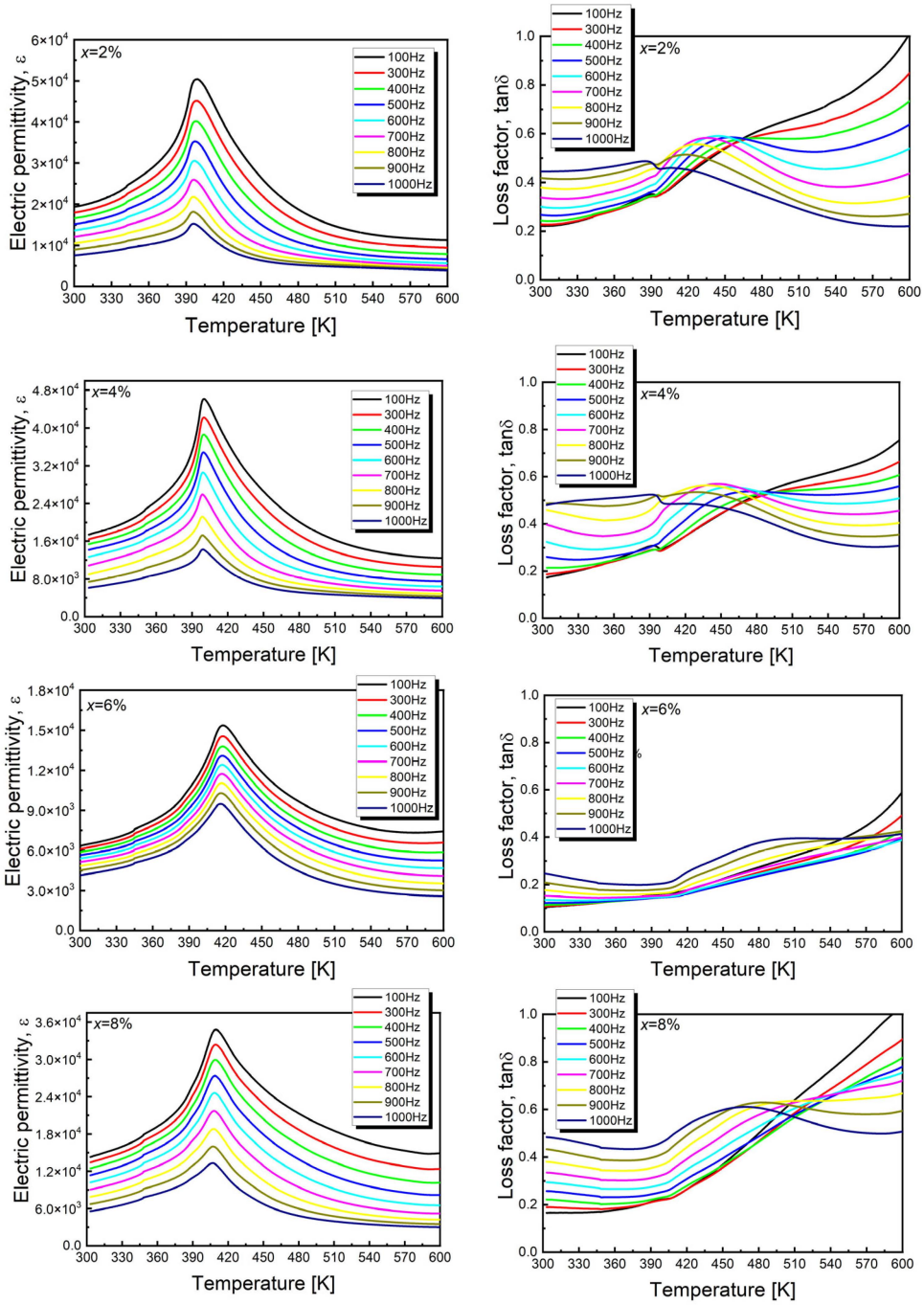

Figure 7. Temperature dependence of electrical permittivity and dielectric loss tangent as a function of temperature and field measurement frequency for ceramics: pure BLT4 and BLT4 ceramics modified with special glass.

4. Conclusions

The microstructure, crystalline structure, and dielectric properties of $Ba_{0.996}La_{0.004}Ti_{0.999}O_3$ ceramics modified with different content of lead-boron special glass were investigated. The additions of special glass caused distinct changes in microstructure. With the increase in the content of the special glass additive, a decrease in grain size is observed. Moreover, the grains are more densely packed. The structure of all the investigated samples was found to be tetragonal, revealing a P4mm space group characteristic of pure $BaTiO_3$ compound. The lattice parameters were weakly dependent on the glass concentration. The addition of glass caused a decrease in the value of electrical permittivity across the entire consid-

ered temperature range and a slight increase in the value of the dielectric loss tangent. However, it should be noted that both values remain attractive for potential applications. Furthermore, this modification enhances dielectric dispersion across all temperature ranges investigated, which is highly valuable for electromagnetic wave absorbers, as mentioned in the introduction.

Author Contributions: Conceptualization, B.W.-D.; methodology, B.W.-D. and K.O.; software, M.A.-H. and R.P.; validation, M.A.-H. and J.M.; formal analysis, M.A.-H.; investigation, M.A.-H. and T.P.; resources, B.W.-D.; data curation, B.W.-D.; writing—original draft preparation, M.A.-H. and J.M.; writing—review and editing, M.A.-H., B.W.-D. and J.M.; visualization, K.O., B.W.-D., T.P. and M.A.-H.; supervision, M.A.-H.; funding acquisition, B.W.-D. All authors have read and agreed to the published version of the manuscript.

Funding: This research received no external funding.

Data Availability Statement: The original contributions presented in the study are included in the article, further inquiries can be directed to the corresponding author.

Conflicts of Interest: The authors declare no conflicts of interest.

References

1. Sumona, H.J.; Sultan, M.S.; Urmi, S.A.; Gafur, M.A. Investigation of structural, electrical and optical properties of lanthanum and zirconium doped barium titanate ceramics. *Mater. Sci. Eng. B* **2023**, *298*, 116844. [CrossRef]
2. Wang, Y.; Shi, S.; Dong, Q.; Xu, C.; Zhu, S.; Zhang, X.; Chow, Y.T.; Wang, X.; Zhang, G.; Zhu, L.; et al. Electrospun lanthanum-doped barium titanate ceramic fibers with excellent dielectric performance. *Mater. Charact.* **2021**, *172*, 110859. [CrossRef]
3. Zeng, L.; Yang, D.; Li, Z.; Xiong, W.; Hao, M.; Ma, H.; Yuan, H.; Cui, J. Microstructural changes and properties of $La_xBa_{(1-x)}(Zr_{0.1}Ti_{0.9})O_3$ multilayer dielectric ceramics via digital light processing. *Ceram. Int.* **2024**, *50*, 19402–19411. [CrossRef]
4. Kaur, S.; Karol, V.; Kumar, P.; Kaur, G.; Sharma, P.; Saroa, A.; Singh, A. Energy build-up factors estimation for $BaZr_{0.10}Ti_{0.90}O_3$, $Ba_{0.90}La_{0.10}TiO_3$ and $Ba_{0.90}La_{0.10}Zr_{0.10}Ti_{0.90}O_3$ ceramics in shielding applications. *Nucl. Eng. Technol.* **2024**, *56*, 1822–1829. [CrossRef]
5. Wodecka-Dus, B.; Plonska, M.; Czekaj, D. Synthesis, microstructure and the crystalline structure of the barium titanate ceramics doped with lanthanum. *Arch. Metall. Mater.* **2013**, *58*, 1305–1308. [CrossRef]
6. Wodecka-Duś, B.; Adamczyk-Habrajska, M.; Goryczka, T.; Bochenek, D. Chemical and physical properties of the BLT4 ultra capacitor—A suitable material for ultracapacitors. *Materials* **2020**, *13*, 659. [CrossRef]
7. Wodecka-Duś, B.; Kozielski, L.; Makowska, J.; Bara, M.; Adamczyk-Habrajska, M. Fe-Doped Barium Lanthanum Titanate as a Competitor to Other Lead-Free Piezoelectric Ceramics. *Materials* **2022**, *15*, 1089. [CrossRef]
8. Ravanamma, R.; Ravi, N.; Kummara, V.K.; Khaerudini, D.S.; Kumar, K.U.; Sreenivasa Kumar, G.; Nanda Kumar Reddy, N. Yttria activated lanthanum-barium titanate ceramic electrode for fast charging supercapacitor applications. *J. Mol. Struct.* **2023**, *1294*, 136352. [CrossRef]
9. Prohinig, J.M.; Kuegler, P.; Reichmann, K.; Hutter, H.; Bigl, S. The interaction of oxygen with manganese and its effect on surface state properties in PTCR $BaTiO_3$. *J. Eur. Ceram. Soc.* **2022**, *42*, 2827–2835. [CrossRef]
10. Leng, S.; Cheng, H.; Zhang, R.; Gao, C.; Li, Z. Electrical properties of La-Mn-codoped $BaTiO_3(Bi_{0.5}Na_{0.5})TiO_3$ lead-free PTCR ceramics. *Ceram. Int.* **2021**, *47*, 30963–30968. [CrossRef]
11. Rajib, M.; Shuvo, M.A.I.; Karim, H.; Delfin, D.; Afrin, S.; Lin, Y. Temperature influence on dielectric energy storage of nanocomposites. *Ceram. Int.* **2015**, *41*, 1807–1813. [CrossRef]
12. Reavley, M.J.H.; Guo, H.; Yuan, J.; Ng, A.Y.R.; Ho, T.Y.K.; Tan, H.T.; Du, Z.; Gan, C.L. Ultrafast high-temperature sintering of barium titanate ceramics with colossal dielectric constants. *J. Eur. Ceram. Soc.* **2022**, *42*, 4934–4943. [CrossRef]
13. Zhu, C.; Cai, Z.; Cao, X.; Fu, Z.; Li, L.; Wang, X. High-dielectric-constant nanograin $BaTiO_3$-based ceramics for ultra-thin layer multilayer ceramic capacitors via grain grading engineering. *Adv. Powder Mater.* **2022**, *1*, 100029. [CrossRef]
14. Gerson, R.; Marshall, T.C. Dielectric breakdown of porous ceramics. *J. Appl. Phys.* **1959**, *30*, 1650–1653. [CrossRef]
15. Yu, J.; Jiang, Q.; Jia, Q.; Zhang, L.; Chiu, W.; Zeng, H. Designing a glass nanoshell on barium titanium trioxide to suppress nanocrystal growth during sintering for fine-grain dielectric ceramics. *J. Mater.* 2024; *in press*. [CrossRef]
16. Manoharan, M.P.; Zou, C.; Furman, E.; Zhang, N.; Kushner, D.I.; Zhang, S.; Murata, T.; Lanagan, M.T. Flexible glass for high temperature energy storage capacitors. *Energy Technol.* **2013**, *1*, 313–318. [CrossRef]
17. Wei, J.; Shang, F.; Zhang, H.; Zhu, G.; Zhao, Y.; Chen, G.; Ye, Z.G.; Xu, J. Improving the energy storage performance of batio$_3$ based glass ceramics by reconstituting glass network structure via electronegativity tuning. *J. Mater.* 2024; *in press*. [CrossRef]
18. Wang, J.; Xin, Z.; Hao, H.; Wang, Q.; Sun, X.; Liu, S. Reinforced dielectric properties and energy storage performance of $BaO–Na_2O–Nb_2O_5–SiO_2–TiO_2–ZrO_2$ dielectric glass ceramics. *Ceram. Int.* **2024**, *50*, 17283–17290. [CrossRef]
19. Belova, L.A.; Goltzov, Y.I.; Prokopalo, O.I.; Rayevsky, I.P. Preparation of semiconducting $BaTiO_3$ ceramics via liquid-phase doping. *Izv. Akad. Nauk. SSSR Neorg. Mater.* **1986**, *22*, 1004–1008.

20. Freidenfel'd, E.Z.; Klyaine, R.Z.; Bogomolov, A.A. Pyroelectric properties of $PbTiO_3$-based ceramics with glass additions. *Izv. Akad. Nauk. Latv. SSR Ser. Khim.* **1987**, *6*, 655–657.
21. Howng, W.Y.; Cutchenon, C. Electrical properties of semiconducting $BaTiO_3$ by liquid-phase sintering. *Am. Ceram. Soc. Bull.* **1983**, *62*, 231–233.
22. Grossman, D.G.; Isard, J.O. Lead Titanate Glass Ceramics. *J. Am. Ceram. Soc.* **1969**, *52*, 230–231. [CrossRef]
23. Yanchevskii, O.Z.; V'yunov, O.I.; Belous, A.G. Fabrication and Properties of Semiconducting Barium Lead Titanate Ceramics Containing Low-Melting Glass Additions. *Inorg. Mater.* **2003**, *39*, 645–651. [CrossRef]
24. Pisarski, W.A.; Goryczka, T.; Wodecka-Duś, B.; Płońska, M.; Pisarska, J. Structure and properties of rare earth-doped lead borate glasses. *Mater. Sci. Eng. B* **2005**, *122*, 94–99. [CrossRef]
25. Ziemba, B. *Technologia Szkła*; Wydawnictwo Arkady: Warszawa, Poland, 1987; Volume 1.
26. Prasad, R.N.A.; Siva, B.V.; Neeraj, K.; Mohan, N.K.; Rojas, J.I. Influence of modifier oxides on spectroscopic features of Nd_2O_3 doped PbO-Ro_2O_3-WO_3–B_2O_3 glasses (with Ro_2O_3 = Sb_2O_3, Al_2O_3, and Bi_2O_3). *J. Lumin.* **2020**, *223*, 117171. [CrossRef]
27. Abdel-Khalek, E.K.; Mohamed, E.A.; Salem, S.M.; Kashif, I. Structural and dielectric properties of (100–x)$B_2O_{3-(x/2)}Bi_2O_3$-$_{(x/2)}Fe_2O_3$ glasses and glass-ceramic containing $BiFeO_3$ phase. *J. Non-Cryst. Solids* **2018**, *492*, 41–493. [CrossRef]
28. Shelby, J.E. *Introduction to Glass Science and Technology*; Royal Society of Chemistry: Cambridge, UK, 2005.
29. Hozer, L. *Półprzewodnikowe Materiały Ceramiczne Z Aktywnymi Granicami Ziarn*; PWN: Warszawa, Poland, 1990.
30. Rao, K.S.; Kumar, V.R.; Veeraiah, N. Dielectric, magnetic and spectroscopic properties of Li_2O–WO_3–P_2O_5 glass system with Ag_2O as additive. *Mater. Chem. Phys.* **2008**, *111*, 283–292. [CrossRef]
31. Salem, S.M. Effect of iron on the electrical properties of lead bismuth glasses. *J. Mater. Sci.* **2009**, *44*, 5760–5767. [CrossRef]
32. Upender, G.; Devi, C.S.; Mouli, V.C. Role of WO_3 on DC conductivity and some optical properties of TeO_2 based glasses. *Mater. Res. Bull.* **2012**, *47*, 3764–3769. [CrossRef]
33. Han, J.; He, F.; Wang, L.L.; Zhang, L.X.; Ye, C.Q.; Xie, J.L.; Mei, S.X.; Jin, M.F. Effect of WO_3 on the structure and properties of low sintering temperature and high strength vitrified bonds. *J. Alloys Compd.* **2016**, *679*, 54–58. [CrossRef]
34. Singh, G.P.; Kaur, P.; Kaur, S.; Singh, D.P. Role of WO_3 in structural and optical properties of WO_3–Al_2O_3–PbO–B_2O_3 glasses. *Phys. B* **2011**, *406*, 4652–4656. [CrossRef]
35. Iordanova, R.; Milanova, M.; Aleksandrov, L.; Khanna, A. Structural study of glasses in the system B_2O_3-Bi_2O_3-La_2O_3-WO_3. *J. Non-Cryst. Solids* **2018**, *481*, 254–259. [CrossRef]
36. Ali, A.A.; Fathi, A.M.; Ibrahim, S. Material characteristics of WO_3/Bi_2O_3 substitution on the thermal, structural, and electrical properties of lithium calcium borate glasses. *Appl. Phys. A* **2023**, *129*, 299. [CrossRef]
37. Pisarska, J.; Wodecka-Duś, B.; Płońska, M.; Goryczka, T.; Pisarski, W.A. Glass characterization in PbO–B_2O_3–Al_2O_3–WO_3 system. *Arch. Nauk. O. Mater.* **2004**, *25*, 193–202.
38. Wodecka-Dus, B.; Adamczyk, M.; Goryczka, T.; Dzik, J.; Radoszewska, D.; Kozielski, L.; Bochenek, D. The technology and structural properties of special glass modified $(Ba_{0.6}Pb_{0.4})TiO_3$ ceramics. *Arch. Metall. Mater.* **2016**, *61*, 1761–1766. [CrossRef]
39. Wodecka-Duś, B.; Adamczyk-Habrajska, M.; Goryczka, T.; Radoszewska, D.; Feliksik, K.; Kozielski, L. Electric and dielectric properties of $(Ba_{0.6}Pb_{0.4})TiO_3$ ceramics modified with special glass in the range of phase transition. *Process. Appl. Ceram.* 2018; 12, 129–135. [CrossRef]
40. Honma, T.; Maeda, K.; Nakane, S.; Shinozaki, K. Unique properties and potential of glass-ceramics. *J. Ceram. Soc. Jpn.* **2022**, *130*, 545–551. [CrossRef]
41. Fu, L.; Engqvist, H.; Xia, W. Glass–Ceramics in Dentistry: A Review. *Materials* **2020**, *13*, 1049. [CrossRef]
42. Ali, A.A.; Ibrahim, S.; Ahmed, E.M.; Rammah, Y.S. Influence of WO_3 on gamma radiation shielding efficiency, physical and optical properties of newly developed Li_2O–CaO–Bi_2O_3–B_2O_3 glasses. *Radiat. Phys. Chem.* **2022**, *198*, 110240. [CrossRef]
43. Andou, M.; Higashida, Y.; Shibata, N.; Takeuchi, H.; Kasashima, T.; Ohbayashi, K. Control of dispersion frequency of $BaTiO_3$-based ceramics applicable to thin absorber for millimeter electromagnetic wave. *J. Eur. Ceram. Soc.* **2006**, *26*, 2175–2178. [CrossRef]
44. Li, W.; Yu, Z.; Wen, Q.; Feng, Y.; Fan, B.; Zhang, R.; Riedel, R. Ceramic-based electromagnetic wave absorbing materials and concepts towards lightweight, flexibility and thermal resistance. *Int. Mater. Rev.* **2023**, *68*, 487–520. [CrossRef]
45. Li, X.; Yuan, G.; Zheng, M.; Li, R.; Meng, Z.; Guo, J.; Zhou, G. Fabrication and electromagnetic wave absorption property of quartz ceramics with a gradient distribution of $BaTiO_3$. *Ceram. Int.* **2019**, *45*, 5965–5970. [CrossRef]
46. Yang, Y.; Kulandaivel, A.; Mehrez, S.; Mahariq, I.; Elbadawy, I.; Mohanavel, V.; Jalil, A.T.; Saleh, M.M. Developing a high-performance electromagnetic microwave absorber using $BaTiO_3$/CoS_2/CNTs triphase hybrid. *Ceram. Int.* **2023**, *49*, 2557–2569. [CrossRef]
47. Li, S.; Sheen, J.; Jang, S.; Bhalla, A.; Croos, L. Quasi lumped parameter method for microwave measurements of dielectric dispersion in ferroelectric ceramics. *Ferroelectr. Lett. Sect.* **1993**, *16*, 21–32. [CrossRef]
48. Kazaoui, S.; Ravez, J.; Maglione, M.; Goux, P. Dielectric relaxation in crystals and ceramics derived from $BaTiO_3$. *Ferroelectrics* **1992**, *126*, 203–208. [CrossRef]

49. Wodecka-Duś, B. *Właściwości Perowskitowej Ceramiki Ferroelektrycznej Na Bazie Tytanianu Baru*; Wydawnictwo Uniwersytetu Śląskiego: Katowice, Poland, 2017.
50. Cross, L.E. Relaxor Ferroelectrics. *Ferroelectrics* **1987**, *76*, 241–267. [CrossRef]